M. MIČIAN©[1], M. FRÁTRIK©[1*], J. BÁRTA©[2]

INVESTIGATION OF BEAM WELDING TECHNOLOGIES EFFECT ON THE PROPERTIES OF WELDED JOINTS OF S960MC STEEL

The work is focused on welding of fine-grained ultra-high-strength steel S960MC by laser beam welding and electron beam welding technologies. For a given type of steel, when the heat input is exceeded, the mechanical properties of welded joints will deteriorate. As a result, using beam welding technologies to limit the amount of heat input is recommended. Several butt welds were made, and mechanical tests and macroscopic analyses were performed to determine the impact of welding parameters on mechanical properties. Using beam welding technologies, the value of heat input was reduced by up to 73% compared to gas metal arc welding. When compared to a gas metal arc welded joint, the width of the soft zone was reduced by 69 to 79%. This resulted in a considerable reduction in the width of the soft zone, which was reflected in a 24% increase in yield strength and a 23% increase in tensile strength compared to gas metal arc welding.

Keywords: laser beam welding; electron beam welding; S960MC; softening effect; UHSS

1. Introduction

The share of high-strength steels in the global steel market is growing every year. The reason is not only the ever-growing automotive industry, which consumes up to 70% of the world's high-strength steel production, but also the general requirement to reduce the weight of structures in other industries. For this reason, production of high-strength steels is expected to almost double in 2027 compared to 2019 [1]. The steel market currently offers several types of high-strength steels, which differ in mechanical properties, method of production, chemical composition, or various specific properties. High Strength Low Alloyed (HSLA) steels account for the largest, more than 50%, of the world's total production of high-strength steels [2].

HSLA steels have undergone significant development in recent decades, resulting in new types of steels with increased yield strength (YS). The essence of these steels is a suitable combination of applied strengthening mechanisms, which, unlike other types of steels, are not based on a gradual increase of carbon content and alloying elements. Primarily, a grain boundary strengthening is used, which as the only strengthening mechanism allows the strength of the material to increase without a significant decrease in ductility [3]. In combination with precipitation strengthening with (Ti, Nb) (C, N) type particles and dislocation strengthening, high-strength steel with good ductility and cold formability is formed [4-6]. In order to apply all the mentioned strengthening mechanisms, it is necessary to use a production process consisting of controlled rolling and controlled cooling – thermo-mechanically controlled process (TMCP).

Among the biggest issues in welding these types of steels are hydrogen induced cracking (HIC) and softening. Cracking may appear in conditions where the cooling rate is too high (e.g. wet welding) [7,8]. However, since the current TMCP steels are more resistant to HIC, the limitations in the welding process are mainly aimed at suppressing the formation of the soft zone in the HAZ [9]. This phenomenon is generally known as the softening effect and is observed for materials formed by unstable bainite and martensite phases. The cause are irreversible changes in microstructure of base material in areas of the HAZ caused by the heat from welding process. The reason is a decrease in the strengthening effects when exposed to high temperatures, which is characteristic of the above-mentioned strengthening mechanisms applied to the steel. While in case of grain boundary strengthening, the decrease in YS is observed only after the austenitizing temperature is reached (increase in austenitic grain), in case of dislocation strengthening there is a significant decrease in the dislocation density and the related decrease in the strengthening effect already at temperatures above 400°C [10-13].

1 UNIVERSITY OF ŽILINA, FACULTY OF MECHANICAL ENGINEERING, UNIVERZITNÁ 8215/1, 010 26 ŽILINA, SLOVAK REPUBLIC
2 SLOVAK UNIVERSITY OF TECHNOLOGY, FACULTY OF MATERIALS SCIENCE AND TECHNOLOGY IN TRNAVA, J. BOTTU 2781/25, 917 24 TRNAVA, SLOVAK REPUBLIC

* Corresponding author: martin.fratrik@fstroj.uniza.sk

The coaersing of the (Ti, Nb)(C, N) precipitates, which also contribute to the decrease in the YS, also partially contributes to the softening effect [14]. The most significant decrease in hardness occurs in areas between A_{c3}-A_{c1} temperatures and in areas below A_{c1}, where no recrystallization occurs but the microstructure is affected by tempering of bainite and martensite. Studies focused on the weldability of TMCP steels show a significant effect of heat input and cooling rate on the resulting mechanical properties of welded joints [15-19]. At higher values of heat input, the risk of decrease in strength of the welded joint appears. The thickness of the welded material must be also considered when assessing the impact of the soft zone width on the strength. As a result, the relative thickness of the soft zone (X_{SZ}) is calculated, which is calculated as the ratio of the soft zone width to the material thickness. When welding sheets of larger thicknesses, there is no decrease in mechanical properties even at higher values of heat input [17,20,21]. Problems occur when welding thin sheets, where there is insufficient heat transfer from the weld area. Therefore, it is recommended to minimize the heat input when welding the given steel types, to minimize the relative thickness of the soft zone. Studies have shown that sufficient narrowing of the soft zone will affect the weld by the constraint effect. Material with higher strength surrounding the softened HAZ creates a hydrostatic stress by the means of constraint boundary condition, which increases the joint strength and ductility [21-24].

The issue of welding thin sheets of TMCP steels using the GMAW method has been addressed, for example, by Jambor et al. [15] and Mičian et al. [16]. These studies investigated the influence of the welding process on the resulting mechanical properties of welded joints, which, despite the significant heat input decrease, did not reach the strength required by the standards. One of the solutions to this issue may be the application of technologies using concentrated energy sources such as laser beam welding and electron beam welding [17,25-27]. The mentioned technologies achieve higher energy density compared to arc welding technologies. The decrease in heat input will significantly affect the width of the softened area which reduces the decrease in the strength of welded joints [28].

The purpose of this work is to assess the influence of beam welding technologies on the properties of the soft zone in the HAZ as well as the influence of the width of the soft zone on the resulting mechanical properties of welded joints. Due to the character of the fusion zone and the low heat input of beam welding technologies, a significant narrowing of the soft zone is expected. For a more detailed comparison and understanding of the results, they will be compared with existing welded joints welded by GMAW and MCAW technologies.

2. Materials and methods

2.1. Experimental material

The base material used to make the welded joints was structural steel Strenx 960 MC (SSAB AB, Sweden) with thickness of 3 mm. The sheet metal was produced by a thermo-mechanical controlled process (TMCP), which in combination with suitable chemical composition leads to the formation of a fine-grained microstructure. The microstructure of the steel consists by a mixture of fine-grained bainite, martensite and tempered martensite (Fig. 1).
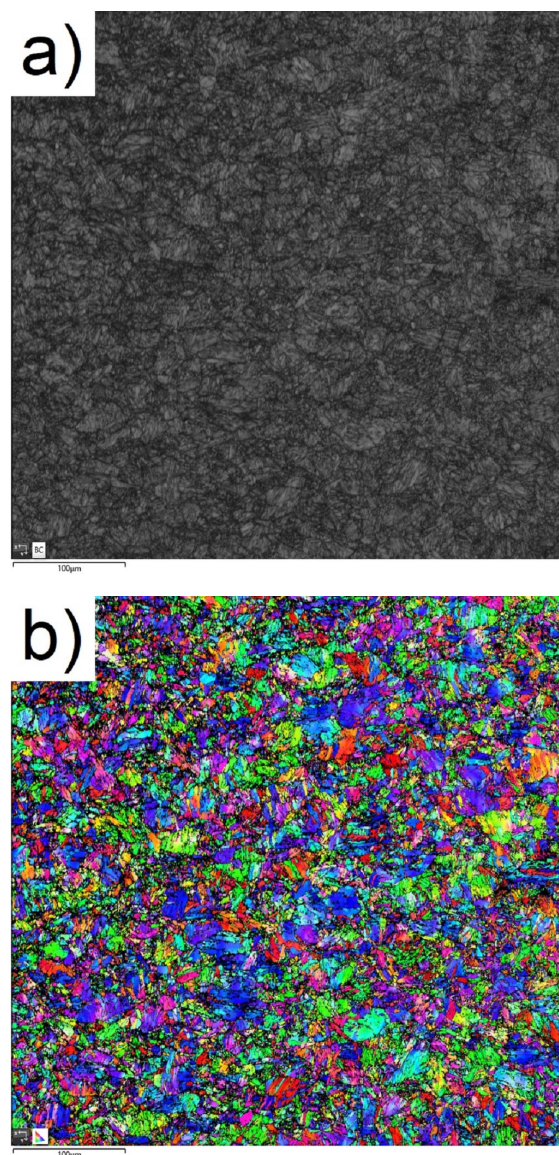

Fig. 1. Martensite-bainitic structure (a) and EBSD grain size analysis (b) of tested S960MC steel (HV 20 kV, step size 0,2 um)

Mechanical properties of the steel according to the inspection certificate are shown in TABLE 1. The chemical composition of the steel based on the inspection certificate from the manufacturer is shown in TABLE 2.

TABLE 1

Mechanical properties of S96MC according to the inspection certificate

$R_{p0,2}$ [MPa]	R_m [MPa]	A [%]	CET/CEV	KV −40°C [J]
1018	1108	6.7	0.28/0.51	32

Chemical composition of S960MC according to the inspection certificate (wt.%)

C	Si	Mn	P	S	Al	Nb	V
0.085	0.18	1.06	0.01	0.003	0.036	0.002	0.007
Ti	Cu	Cr	Ni	Mo	N	B	
0.026	0.01	1.08	0.07	0.109	0.005	0.0015	

The filler material used in the laser beam welding with the filler material variant was Union X96 L-MC wire with diameter of 1 mm (Voestalpine, Austria) with classification G89 5 M21 Mn4Ni2.5CrMo according to STN EN ISO 16834-A. The chemical composition of the filler material guaranteed by the manufacturer is given in TABLE 3.

TABLE 3

Chemical composition of Union X96 L-MC according to manufacturer (wt.%)

C	Si	Mn	Cr	Ni	Mo
0.12	0.8	1.9	0.45	2.35	0.55

2.2. Welding procedure

Welded joints were made using laser beam welding (LBW) and electron beam welding (EBW) technologies. Sheets of
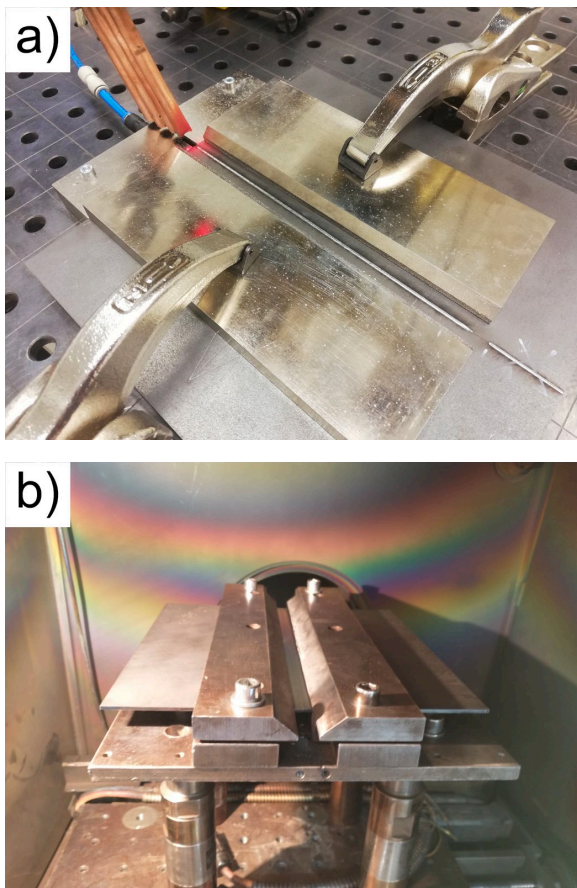

a)

b)

Fig. 2. Welding of experimental welded joints by LBW (a) and EBW (b)

S960MC steel with dimensions $150 \times 300 \times 3$ mm were welded for both technologies as closed square butt joints (no root opening). The welding edges were thoroughly cleaned and degreased before welding. The laser-welded joints welded without filler material marked as LBW-S2 (Standard 2), welded with filler material marked as LBW-FM, and welded without filler material with additional dressing marked as LBW-D (Dressing) were made on TRUMPF TruDisk 4002 (TRUMPF, Germany) device. The laser-welded joint welded without filler material marked as LBW-S1 (Standard 1) was made on YLR 4500 (IPG Photonics, USA) device. All joints were shielded by 4.6 argon (the weld root was protected with helium shielding gas). The welding process of LBW-S2 variant is shown in Fig. 2a. The LBW-FM weld was welded using a filler material with wire feed speed 0.5 m.min^{-1}. The EBW welded joint was made on the PZ EZ4 (First welding company Inc., Slovakia) device. The welded parts were clamped in the jig without stitching tack welding (Fig. 2b).

Welding parameters for LBW are shown in TABLE 4 and welding parameters for EBW are shown in TABLE 5.

TABLE 4

Welding parameters of LBW welded joints

Weld	Power [W]	Travel speed [mm.s^{-1}]	Focus [mm]	Gas flow [l.min^{-1}]	Heat input [kJ.cm^{-1}]
LBW-S1	4250	30	+3.5	6	1.41
LBW-S2	2000	20	−1.0	30	1.00
LBW-FM	2000	18	−1.0	30	1.11
LBW-D*	2000	20	−1.0	30	1.00
LBW-D**	2000	20	+10.0	30	1.00
* – 1st layer (weld); ** – 2nd layer (additional dressing)					

TABLE 5

Welding parameters of EBW welded joint

Weld	Accelerating voltage [kV]	Welding current [mA]	Travel speed [mm.s^{-1}]	Chamber pressure [Pa]	Heat input [kJ.cm^{-1}]
EBW	55	100	40	<1,2.10^{-2}	1.37

The heat input for electron beam welding was calculated according to Eq. (1) and for laser beam welding according to Eq. (2).

$$Q_{EBW} = \frac{60 \cdot V \cdot I}{1000 \cdot v} \qquad (1)$$

$$Q_{LBW} = \frac{60 \cdot W}{v} \qquad (2)$$

2.3. Mechanical testing and macroscopic analysis

After the welding process, test specimens were taken from all welds for a tensile test, a hardness test, a bend test, and structural analysis. For the purpose of the tensile test, two samples were taken from each welded joint, from which the average values of yield strength, tensile strength, and elongation were

determined. Dimensions of the test specimen were made according to the STN EN ISO 4136 standard to perform the tensile strength test. Measurements were realized on an INSTRON 5985 (Instron, USA) testing device.

The bend test was performed on four samples from each welded joint according to STN EN ISO 5173, where two samples were loaded from the root side (TRBB) and two samples from the face side (TFBB) of the weld. The essence of the test was the three-point bending deformation of the test specimen by load former up to the prescribed bending angle or until the detection of cracking. The diameter of the load former was determined to be 35 mm according to the ductility of the base material. Eq. (3) describes the calculation of the load former diameter ($\o d$). The test was performed on a WDW 20 (Jinan Kason testing equipment CO., LTD, China) testing device.

$$\o d = \frac{100 \cdot specimen\ thickeness\,(\mathrm{mm})}{A\,(\%)} +$$
$$- specimen\ thickness\,(\mathrm{mm}) \qquad (3)$$

The linear hardness measurements were performed by the Vickers method (HV0.1) on an Innovatest Nexus 4300 (Innovatest, The Netherlands) testing device. Based on these measurements, the width of the soft zones was evaluated. The soft zone is considered to be the HAZ area with a hardness drop below 90% of the hardness of the base material. This criterion is based on literature review and has also been confirmed by physical simulations [8]. An area where hardness is less than the selected criterion value is considered the soft zone. The line was guided through the center of the material thickness, the individual indentations being spaced 100 μm apart. The total amount of 121 measurements for each welded joint were made.

The macrostructures of the welded joints were analyzed by a Neophot 2 (Carl Zeiss, Germany) device. All samples were etched with 2% Nital.

3. Results and discussion

3.1. Tensile test

The average values of the yield strength (YS), tensile strength (TS), and elongation for each welded joint and base material are shown in TABLE 6. The values for the base material are based on our own measurements and will serve as the reference values for further calculations. Since the given material does not show a significant yield point, the value of the yield strength R_e had to be replaced by the offset yield point (or proof stress) $R_{p0.2}$, which is taken as the stress where 0.2% plastic deformation occurs. The yield point was for all welded joints determined graphically from the working diagram of the tensile test. Fig. 3 shows the fracture profiles of all welded joints. The fracture/initial crack was for every welded joint localized to the sub-critical HAZ (SCHAZ). The same results were observed by Mičian et al. [8], or by Amraei et al. [29].
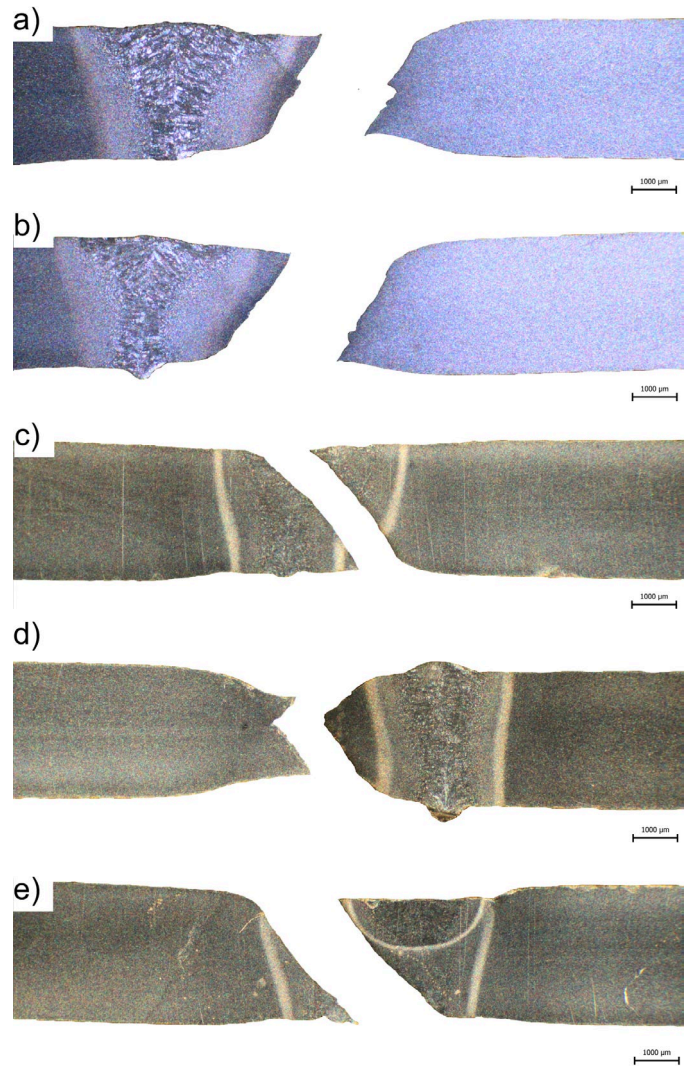

Fig. 3. Fracture profiles made after the tensile test: (a) EBW, (b) LBW-S1, (c) LBW-S2, (d) LBW-FM, (e) LBW-D

TABLE 6

Mechanical properties of the evaluated welded joints of S960MC steel

Specimen	$R_{p0.2}$ [MPa]	Average value $R_{p0.2}$ [MPa]	R_m [MPa]	Average value R_m [MPa]	A [%]
Base material	1007	1007	1092	1092	7,9
EBW	993	989	1016	1017	2,2
	986		1019		
LBW-S1	997	998	1027	1026	2,3
	999		1025		
LBW-S2	1078	1079	1153	1152	4,1
	1079		1152		
LBW-FM	998	998	1083	1085	6,0
	998		1087		
LBW-D	1089	1091	1130	1129	2,47
	1092		1127		

Results showed that the yield strength and the tensile strength reached the required minimum values of the base material. These were set by the standard STN EN ISO 10149-2 at

960 MPa for the YS and 980 MPa for the TS. It is also possible to observe a significant elongation decrease compared to the base material.

3.2. Bend test

The bend test showed sufficient deformation properties for all laser welded joints. In the case of EBW welded joint, cracks appeared during the test on one of the test specimens (Fig. 4), based on which it is possible to state unsatisfactory deformation properties of the given welded joint. A crack appeared on the face-loaded sample (TFBB) and the crack was initiated in the SCHAZ.

Fig. 4. Cross-section of the EBW welded joint after the bend test

3.3. Hardness measurements

Hardness measurements were realized to analyze the softening effect in the HAZ. Based on the measured values the width of the soft zone was determined for all welded joints. The character of hardness is similar for all assessed welds and is characterized by a hardness drop in the HAZ. Due to the significantly narrow HAZ and distances between indentations, it is not possible to observe a typical increase in hardness in the fine-grain HAZ (FGHAZ), as is typical for GMAW welded joints [8]. The results of the linear hardness measurements are shown in the Fig. 5.

The largest hardness drop was observed the inter-critical HAZ (ICHAZ) for all samples and reached values from 75% to 78% of base material hardness. The average hardness value of the base material (BM) was 384 HV0.1. Based on this value, the criterion value for the soft zone was set at 346 HV0.1 (90% of the BM hardness value). Based on these measurements, the width of the soft zone was determined for all assessed welds. The soft zone width values are given in TABLE 7.

3.4. Macroscopic analysis

Macroscopic analysis was performed on the cross-sections of welded joints. The images show a narrowing of the HAZ associated with a decrease in heat input for LBW-S2 welded joint compared to LBW-S2 welded joint. It is also possible to
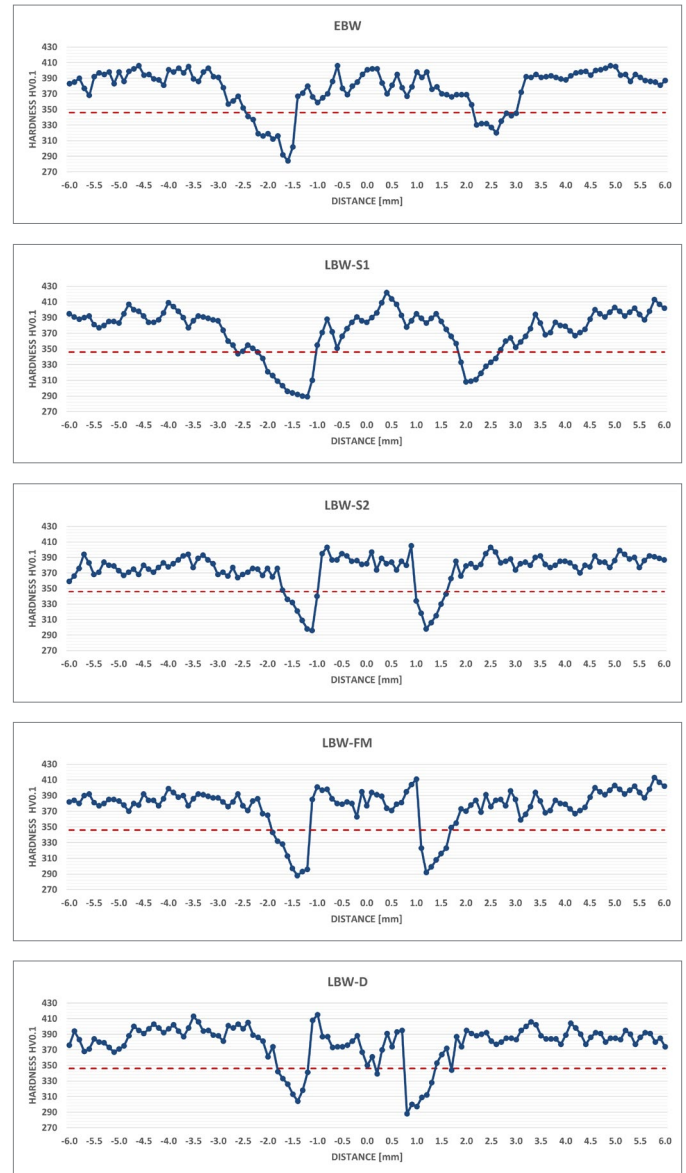

Fig. 5. Linear hardness measurements for all assessed welded joints

TABLE 7

Values of the width of the soft zones and the relative thicknesses of the soft zones (X_{SZ})

Method	Soft Zone [mm]		X_{SZ} [-]
	Left Side of the HAZ	Right Side of the HAZ	
EBW	1.03*	0.85	0.34
LBW-S1	1.10*	0.85	0.37
LBW-S2	0.72*	0.65	0.24
LBW-FM	0.75*	0.62	0.25
LBW-D	0.69*	0.60	0.23

* The side of the weld on which the fracture occurred and from which the X_{SZ} value was calculated.

observe an improvement in the surface (removal of notches) in the variant using a filler material (LBW-FM) and with the variant using additional dressing (LBW-D) compared do variants welded without filler material (LBW-S1, LBW-S2, EBW).
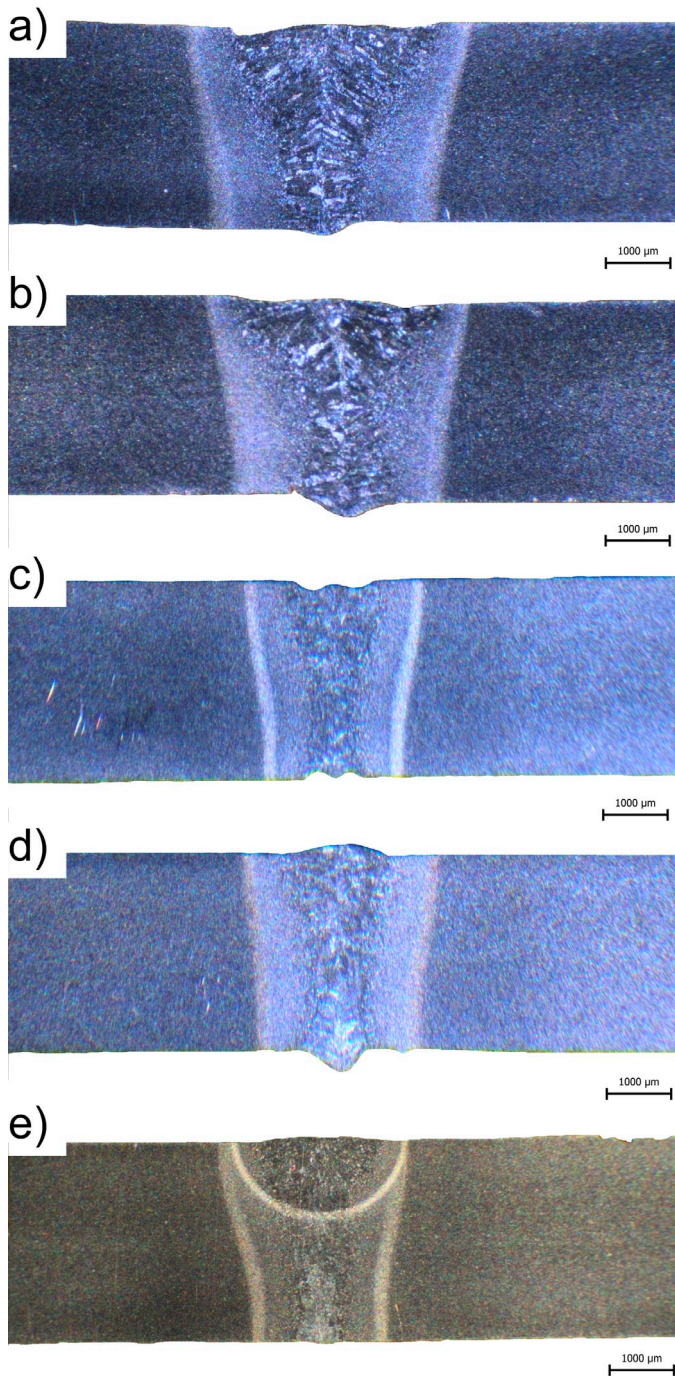
Fig. 6. Macroscopic analyses of welded joints: (a) EBW, (b) LBW-S1, (c) LBW-S2, (d) LBW-FM, (e) LBW-D

3.5. The softening effect for S960MC welded joints

After measuring the width of the soft zone for all LBW and EBW welded joints, the values were converted to the relative thickness of the soft zone parameter. The given parameter was obtained as the ratio of the width of the soft zone to the thickness of the material. Thanks to this recalculation, it will be possible to consider the thickness of the welded material (in this case only a plate with thickness of 3 mm was used). The values of the relative thickness of the soft zone were subsequently compared with the relative values of YS and TS. The values of YS and TS

of the welded joints were recalculated in the used graph with respect to the value of YS and TS of the base material (TABLE 6).

For comparison, the Fig. 7 also shows the values of welded joints welded by GMAW and MCAW technologies. The values of YS, TS and X_{SZ} for these welds (GMAW, MCAW) come from already performed experiments, the results of which were published in Mičian et al. [8]. This comparison makes it possible to observe a significant difference between beam welding technologies and arc welding technologies in all the observed parameters.

The values belonging to YS/TS are connected by a power trendline. Such an expression best describes the effect of the relative thickness of the soft zone on YS/TS of welded joints.
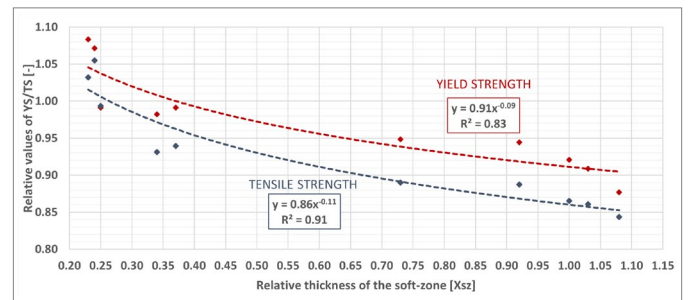

Fig. 7. Influence of the relative thickness of the soft zone (X_{SZ}) on the yield strength (YS) and tensile strength (TS) of the S960MC welded joints

TABLE 8

The values of relative YS/TS and relative thickness of the soft zone [X_{SZ}]

	Relative YS [–]	Relative TS [–]	X_{SZ} [–]
LBW-S1	0.99	0.94	0.37
LBW-S2	1.07	1.04	0.24
LBW-FM	0.99	0.99	0.25
LBW-D	1.08	1.03	0.23
EBW	0.98	0.93	0.34
GMAW-S [16]	0.88	0.84	1.08
GMAW-P [16]	0.91	0.86	1.03
GMAW-CMT [16]	0.92	0.87	1.00
MCAW-S [16]	0.94	0.89	0.92
MCAW-S cooled [16]	0.95	0.89	0.73

* The relative values of YS and TS are calculated from the BM values from TABLE 6.

4. Conclusions

The significant reduction of heat input was achieved using beam welding technologies. The value of heat input was reduced by up to 73% compared to GMAW welding technology [8]. This significant decrease of heat input caused a decrease in the width of the soft zone, which was also reflected in the values of yield strength and tensile strength. These findings are consistent with similar experiments and simulations performed on TMCP steels [23,24,30-33]. The width of the soft zone was reduced by 69%

in the case of EBW, and by up to 79% in the case of LBW, compared to the GMAW-S welded joint. Yield strength and tensile strength reached the required values for all welded joints. In the case of LBW-S2 and LBW-D, the YS and TS values exceeded the values of the base material. It can be concluded that with a sufficiently small value of X_{SZ}, it is possible to achieve YS and TS at the level of base material. It follows that for values of the relative thickness of the soft zone less than 0.65, YS and TS should reach the standard required values applicable to S960MC steel. According to Fig. 7 it can be also seen that the softening effect has a more pronounced effect on a decrease in YS than on a decrease in TS.

REFERENCES

[1] https://www.reportsanddata.com/report-detail/high-strength-steel-market, accessed: 5.6.2022

[2] https://www.grandviewresearch.com/industry-analysis/high-strength-steel-market, accessed: 5.6.2022

[3] S. Endo, N. Nakata, JFE Tech. Rep. **20**, 1-7 (2015).

[4] J. Webel, A. Herges, D. Britz, E. Detemple, V. Flaxa, H. Mohrbacher, F. Mücklich, Metals **10**, 243 (2020). DOI: https://doi.org/10.3390/met10020243

[5] B. Wang, J. Lian, Mater. Sci. Eng. A **592**, 50-56 (2014). DOI: https://doi.org/10.1016/j.msea.2013.10.089

[6] Y. Funakawa, T. Shiozaki, K. Tomita, T. Yamamoto, E. Maeda, ISIJ Int. **44**, 1945-1951 (2004). DOI: https://doi.org/10.2355/isijinternational.44.1945

[7] J. Tomków, A. Świerczyńska, M. Landowski, A. Wolski, G. Rogalski, J. Adv. Sci. Tecnol. Res. **15**, 288-296 (2021). DOI: https://doi.org/10.12913/22998624/140223

[8] J. Tomków, M. Landowski, D. Fydrych, G. Rogalski, Mar. Struct. **81**, 103120 (2022). DOI: https://doi.org/10.1016/j.marstruc.2021.103120

[9] J.H. Kim, J.S. Seo, H.J. Kim, H.S. Ryoo, K.H. Kim, M.Y. Huh, Met. Mater. Int. **14**, 239-245 (2008). DOI: https://doi.org/10.3365/met.mat.2008.04.239

[10] J. Moravec, I. Novakova, J. Sobotka, H. Neumann, Metals **9**, 707 (2019). DOI: https://doi.org/10.3390/met9060707

[11] https://ssabwebsitecdn.azureedge.net/-/media/files/en/strenx/ssab-strenx-welding-brochure-2018.pdf, accessed 9.8.2022

[12] K. Zhang, Z. Li, X. Han, X. Sun, Q. Yong, Microalloying 2015 & Offshore Engineering Steels 2015: Conference Proceedings (2015)

[13] S. Rešković, L. Benić, M. Lovrenić-Jugović, Metals **10**, 294 (2020). DOI: https://doi.org/10.3390/met10020294

[14] P. Gong, E.J. Palmiere, W.M. Rainforth, Acta Mater. **97**, 392-403 (2015). DOI: https://doi.org/10.1016/j.actamat.2015.06.057

[15] M. Jambor, F. Nový, M. Mičian, L. Trško, O. Bokůvka, F. Pastorek, D. Harmaniak, Communications **20**, 4 (2018). DOI: https://doi.org/10.26552/com.C.2018.4.29-35

[16] M. Mičian, M. Frátrik, D. Kajánek, Metals **11**, 2. 305 (2021). DOI: https://doi.org/10.3390/met11020305

[17] C. Schneider,W. Ernst, R. Schnitzer, H. Staufer, R. Vallant, N. Enzinger, Weld. World **62**, 801-809 (2018). DOI: https://doi.org/10.1007/s40194-018-0570-1

[18] F. Hochhauser, W. Ernst, R. Rauch, R. Vallant, N. Enzinger, Weld. World **56**, 77-85 (2012). DOI: https://doi.org/10.1007/BF03321352

[19] Ch. Wen, Z. Wang, X. Deng, G. Wang, R.D.K. Misra, Steel. Res. Int. 1700500 (2018). DOI: https://doi.org/10.1002/srin.201700500

[20] M. Tümer, R. Vallant, F. Warchomicka, N. Enzinger, J. Mater. Eng. Perform. **31**, 6 (2022). DOI: https://doi.org/10.1007/s11665-022-06876-4

[21] M. Amraei, A. Ahola, S. Afkhami, T. Bjork, A. Heidarpour, X.-L. Zhao, Eng. Struct. **198** (2019). DOI: https://doi.org/10.1016/j.engstruct.2019.109460

[22] M. Amarei, T. Skriko, T. Björk, X.-L. Zhao, Thin-Walled Struct. **109**, 227-241 (2016). DOI: https://doi.org/10.1016/j.tws.2016.09.024

[23] W. Maurer, W. Ernst, R. Rauch, R. Vallant, N. Enzinger, Weld. World **59**, 809-822 (2015). DOI: https://doi.org/10.1007/s40194-015-0262-z

[24] D.M. Rodrigues, L.F. Menezes, A. Loureiro, J.V. Fernandes, Numerical study of the plastic behavior in tension of welds in high strength steels, Int. J. Plast. **20**, 1-18 (2004). DOI: https://doi.org/10.1016/S0749-6419(02)00112-2

[25] W. Guo, D. Crowther, J. A. Francis, A. Thompson, Z. Liu, L. Li, Mater. Des. **85**, 534-548 (2015). DOI: https://doi.org/10.1016/j.matdes.2015.07.037

[26] I. Dzioba, T. Pala, Metals **13**, 747 (2020). DOI: https://doi.org/10.3390/ma13030747

[27] J. Górka, Materials **11**, 1192 (2018). DOI: https://doi.org/10.3390/ma11071192

[28] F. Farrokhi, J. Siltanen, A. Salminen, J. Manuf. Sci. Eng. **137** (2015). DOI: https://doi.org/10.1115/1.4030177

[29] M. Amraei, M. Dabiri, T. Björk, T. Skriko, J. Manuf. Sci. Eng. **138**, 121007-1 (2016). DOI: https://doi.org/10.1115/1.4033930

[30] M. Mochizuki, T. Shintomi, Y. Hashimoto, M. Toyoda, Weld. World. **48** (2004). DOI: https://doi.org/10.1007/BF03263396

[31] R. Mai, Z. Jiang, J. Ma, Y. Zhang, Appl. Mech. Mater. **872**, 99-106 (2017). DOI: https://doi.org/10.4028/www.scientific.net/AMM.872.99

[32] G.-B. An, S.-K. Nam, T.-W. Jang, Mater. Sci. Forum. **580-582**, 589-592 (2008). DOI: https://doi.org/10.4028/www.scientific.net/MSF.580-582.589

[33] K.-S. Bang, W.-Y. Kim, Weld. J. **81**, 174-179 (2002).